

# Numerical Simulations of Interacting Gas-Rich Barred Galaxies

I. Berentzen, C.H. Heller & K.J. Fricke ([iberent@uni-sw.gwdg.de](mailto:iberent@uni-sw.gwdg.de))  
*Universitäts-Sternwarte Göttingen, Germany*

E. Athanassoula  
*Observatoire de Marseille, France*

## Abstract.

Using an N-body+SPH code we have performed numerical simulations to investigate the dynamical effects of an interaction between an *initially* barred galaxy and a small spherical companion. In the models described here the small companion passes through the disk of the larger galaxy perpendicular to its plane. The impact positions and times are varied with respect to the evolutionary phase of the bar and disc. The interactions produce expanding ring structures, offset bars, spokes, and other asymmetries in the stars and gas. They also affect the strength and pattern speed of the bar.

## 1. Introduction

The evolution of disc galaxies is driven by both internal and external processes. Internal instabilities in the disc often give rise to the formation of a bar. Bars are a common feature in disc galaxies and by no means an exception, since about 2/3 of all disc galaxies are believed to harbor a bar or oval distortion. Furthermore in the last few years near-infrared observations have given clear indications of an even higher fraction of barred galaxies. The presence of a bar changes both the kinematics and mass (stellar and gas) distributions within the disc and can give rise to dynamical resonances (e.g., Sellwood & Wilkinson, 1993). Similarly, it has become increasingly recognized that interactions with small companions are a frequent and important external agent driving dynamical evolution. Since both these processes are thought to be frequent, it is a reasonable assumption that the interaction between a barred disc galaxy and a small companion is a common event.

The study of Athanassoula et al. (1997), using pure N-body simulations, has demonstrated that a sufficiently massive companion hitting the inner parts of a barred disc galaxy can displace the bar and produce expanding stellar rings. In this work we have included the dissipative effects of a gas component.



## 2. Numerical Methods

For the simulations we use an N-body/SPH code to evolve the stellar and gaseous components of the galaxies. A detailed description of the algorithm can be found in Heller (1995) and Heller & Shlosman (1994). The gravitational forces and neighbor interaction lists were computed using the special purpose hardware GRAPE-3AF. The advantage of the GRAPE hardware, besides its speed, is that it does not set any constraints on the symmetry of the simulations. The adopted units for mass, distance, and time are  $M = 6 \cdot 10^{10} M_{\odot}$ ,  $R = 3$  kpc, and  $\tau = 10^7$  yr, respectively, and the gravitational constant is taken as unity. A fixed gravitational softening length of  $\epsilon = 0.1875$  kpc is used for all particles.

### 2.1. INITIAL CONDITIONS

Both the stellar and gaseous discs are initially setup with a truncated Kuzmin-Toomre projected radial density profile and a  $sech^2$  vertical distribution. The halo and companion have a truncated Plummer profile. The parameters are given in Table 1 and were chosen so as to give a bar unstable model.

Based on the potential of the disc and relaxed halo we assign velocities to the disc particles. The velocity dispersion is derived from the local stability criterion and is corrected for asymmetric drift. The resulting rotation curve has a maximum of  $v_{\max} \approx 200$  km/s and remains flat in the outer disc.

The initial conditions for the interactions are specified by the impact position  $(x_i, y_i)$  with respect to the bar and the impact time  $t_i$ . The impact velocity  $v_i$  of the companion is chosen to be roughly equal to  $4v_{\text{esc}}$ , with  $v_{\text{esc}}$  being the escape velocity from the center of the target system. The orbit is integrated backward for a time period of  $\Delta t = 30$ , which places the companion well outside the halo of the disc system. A more complete description of the procedure for setting up the interaction configuration can be found in Berentzen et al. (1999 a,b). For the simulations in this paper we have chosen two different impact times, one at  $t_i = 60$  and the other at  $t_i = 150$ . As will be shown in the next sections, the former corresponds roughly to the time of the maximum bar strength and the latter to a time when the bar is considerably weaker. We will thus hereafter refer to cases with the first impact time as interactions with a strong bar and to cases with the second one as interactions with a weak bar.

Table I. Initial model parameters

		Type	$N_D$	$M_D$	$a_D$	$R_{\text{cut}}$	$z_0$
<b>Disc</b>	stars	KT	13 500	0.56	1.0	5.0	0.20
	gas	KT	10 000	0.14	1.0	5.0	0.05
<b>Halo</b>	stars	PL	32 500	1.30	5.0	10.0	...
<b>Companion</b>	stars	PL	10 000	0.40	0.195	3.0	...

### 3. Morphological Evolution

#### 3.1. ISOLATED GALAXY

The model was constructed so as to be globally unstable to non-axisymmetric perturbations and forms a large-scale bar in a few disc rotations ( $t_{\text{rot}}$ , measured at disc half-mass radius). The bar reaches its maximum strength at  $t = 60$  or some  $20 t_{\text{rot}}$ . At this time the bar has a major axis length of  $a = 6$  kpc and an axial ratio of  $\sim 3 : 1$ . Both stellar and gaseous trailing spiral arms emerge from the end of the bar. While the stellar arms slowly dissolve and are hardly visible at  $t = 100$ , large spiral features in the gas persist throughout the run. The gas also forms straight off-set shocks at the leading edges of the stellar bar.

Due to the gravitational torque of the bar, the gas is driven towards the center and within two bar rotations some 50 percent of the total gas mass collects in an oval nuclear disc elongated along the bar. As a result of the growing mass concentration at the center the amplitude of the bar decreases, but then settles down to a quasi-steady state as the initial burst of inflow slows down.

The inner regions are connected with the outer disc through two trailing spiral arms, which by way of their shocks feed material inward to the growing central disc. Around the nuclear disc forms another disc which is oriented perpendicular to the bar major axis. This indicates the presence of an ILR, i.e. the existence of an  $x_2$  orbit family. Outside the central region there is a deficiency of gas out to a radius of 3 kpc, where a gas ring forms close to the UHR. A detailed discussion on orbits and resonances in isolated gas-rich barred galaxies can be found in Berentzen et al. (1998).

#### 3.2. CENTRAL PASSAGE

In the model with a strong bar both the stellar and the gaseous components of the bar get torn apart into two fragments. The stellar fragments merge again in about  $3 t_{\text{rot}}$ . The gaseous fragments do not merge as fast,

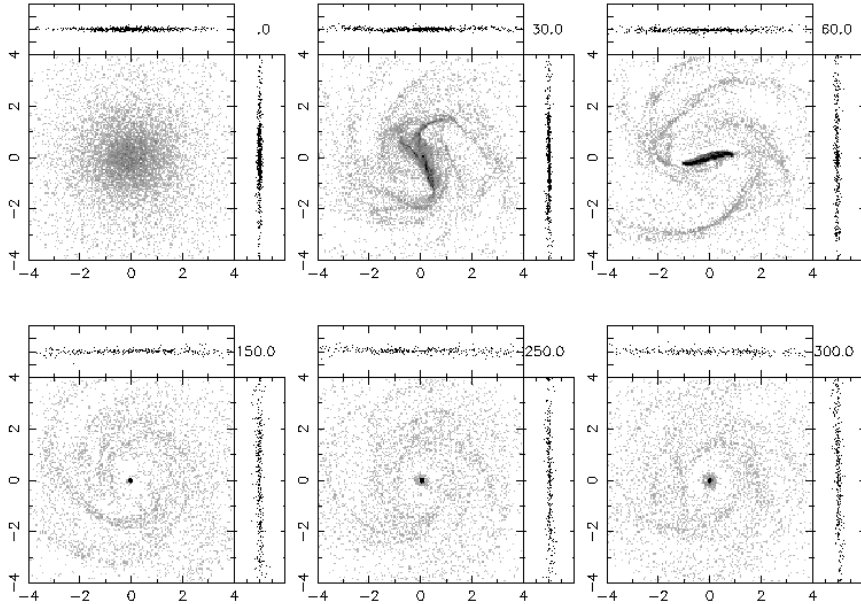
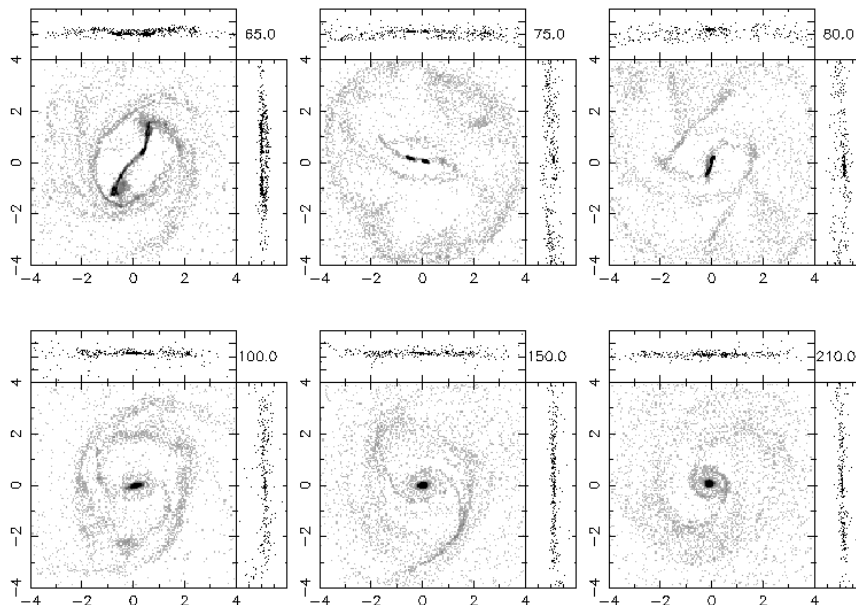


Figure 1. Isolated model. Shown is the evolution of the gaseous disc only.

but flow back and forth inside the bar potential avoiding the center for some  $6 t_{\text{rot}}$  and appear as two separate nuclei, until they finally merge to form a dense nuclear disc. A lower density, more extended circum-nuclear disc forms around the denser nuclear disc as in the isolated model, but with a much larger radius.

The central impact also creates ring-like expanding density waves in the disc, similarly to what happens for non-barred galaxies (Lynds & Toomre, 1976). The first ring reaches as far as half the corotation radius and then fragments, with much of its mass flowing back toward the inner few kpc. A second ring propagating outwards follows the first, with trailing spokes forming between the two. For the weak bar the rings are almost perfectly circular, while for the strong bar they are more asymmetric. One could expect such density enhancements to be accompanied by the formation of bright young blue stars and HII regions.

The expansion velocity of the first ring drops gradually from 88 km/s to roughly 35 km/s. The second ring starts with a lower expansion velocity of 29 km/s, decreasing further to 12 km/s, which is the sound speed of the isothermal gas in the model. With the passage of the two rings the stellar disc is heated up, preventing the formation of a third



*Figure 2.* Central impact with strong bar. Shown is the evolution of the gaseous disc only.

stellar ring. In contrast, more than two rings form in the gas, but from the third onwards they are very weak and dissolve quickly, since they are not supported by an accompanying stellar density enhancement. These rings eventually merge with the existing spiral arm segments.

### 3.3. MINOR AXIS PASSAGE

In these simulations the companion hits the disc along the bar minor axis at a distance of approximately  $r_i = 3.0$  kpc. In both strong and weak bar models the stellar bar gets displaced from the center immediately following the impact to a distance of approximately 3.0 kpc in the direction of the impact point. This offset lasts for a period of roughly  $\Delta t = 0.6$  Gyr.

An expanding circular ring is formed at the impact point, which upon encountering the bar and spiral arms becomes distorted. The ring expands more freely on the side of the bar which is opposite the impact point and also maintains longer its circular shape, before merging with a spiral arm. This merged ring/arm then opens up forming a large spiral feature. On its other side, the ring stays close to the bar. Also a new

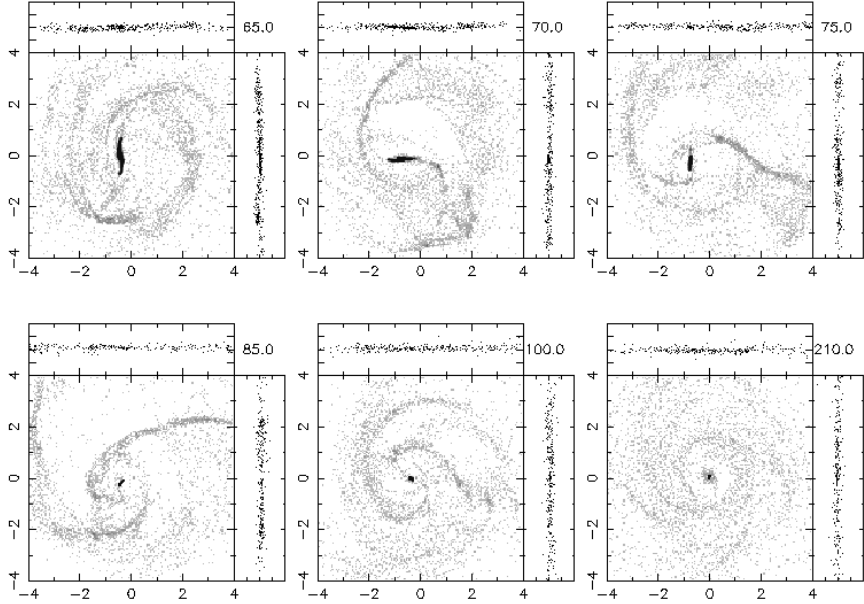


*Figure 3.* Major axis impact with strong bar. Shown is the evolution of the gaseous disc only.

spiral arm segment forms, connected to one end of the still displaced bar.

At the time when the bar is again nearly centered a second ring starts to form, expanding outwards from the impact point. This ring merges with the newly formed spiral arm segment. Between this feature and the large spiral arm there is a noticeable deficiency of both stars and gas.

Similar to the central impact, additional rings form at later times and merge with the many spiral arms that are present, forming spiral segments which wind up and dissolve over time. The final gas morphology is similar to that of the isolated case, even though the stellar bar has been destroyed.

### 3.4. MAJOR AXIS PASSAGE

In these simulations the companion hits the disc on the bar major axis near corotation. Immediately following the passage of the companion through the disc plane, the stellar bar is displaced from the center to a distance of 2.4 kpc in the direction of the impact point .

In general we find the same kind of evolution as in the minor axis impact, though the lengths and orientations of the generated features differ. The most significant difference is that the bar survives the major axis impact. In fact the evolution of the bar strength follows closely that of the isolated case. Again, the final gas configuration is similar to the other models.

## 4. Evolution of the bar

### 4.1. AMPLITUDE OF THE BAR

We have measured the bar strength as defined by the amplitude of the  $m = 2$  Fourier component of the stellar mass distribution in the disc. For models in which the bar gets displaced we trace the center of mass of the stellar bar and measure its amplitude within a radius of 3 kpc from this center. The results are shown in figure 2(a) and (b).

With the central passage the bar is destroyed immediately following the impact of the companion, independent of the bar strength. In the model with the minor axis passage the bar is also destroyed, but its amplitude decreases more slowly over time than in the central passage. Impacts along the bar major axis show the same evolution of the bar strength as in the isolated model.

### 4.2. PATTERN SPEED OF THE BAR

In the isolated model the pattern speed increases linearly with time during the period in which gas is flowing inward. Once the inflow stops the bar quickly settles down to a quasi-steady state and rotates with the constant rate of  $\Omega_p = 0.3\tau^{-1}$ .

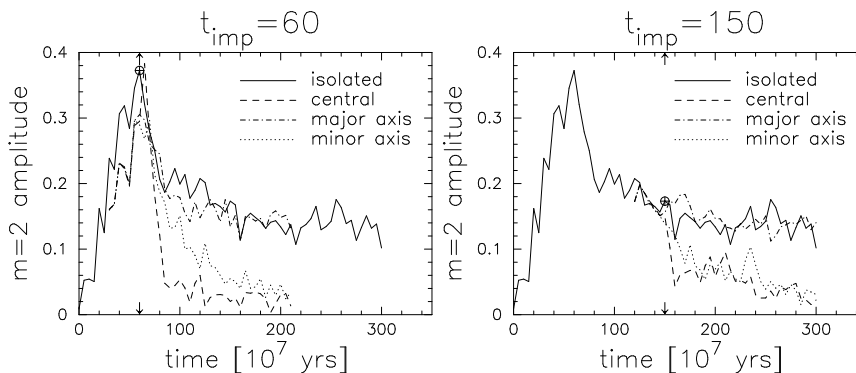


Figure 4. Evolution of bar strength. Models at impact times of (a)  $t = 60$  and (b)  $t = 150$  are shown.

In the case of the central passage, the bar is quickly weakened and it is difficult to follow the pattern speed for more than a few disc rotations after the impact. However, the general trend is that of a slowing down of the bar in both the strong and weak bar models.

In the strong bar minor axis passage the pattern speed increases with time, converging to a value of  $\Omega_p = 0.5$ . In contrast, the weak bar minor axis passage shows little variation of the pattern speed. The major axis passages show the same evolution of pattern speed as in the isolated model.

## 5. Summary

Using N-body/SPH simulations we have examined the effect of a small spherical companion passing through the disc of a gas-rich barred galaxy. The impact position has been varied with respect to the bar and two different impact times have been chosen, corresponding to weak and strong bar cases.

The interaction produces characteristic features like expanding rings, spokes, and an off-centered bar, similar to what has been found in pure N-body simulations. The offset passages lead to a displacement of the bar from the center which lasts for approximately 0.6 Gyr.

While the morphology for several disc rotation times following the impact is drastically altered by the interaction, the overall final state of the bar and disc is similar to that of the isolated case. However, the interaction does change the detailed structure of the gas distribution in the central region and signs of an interaction in the form of asymmetries are left in the outer disc. The bar is not necessarily destroyed by the interaction, even though being temporarily displaced from the center.

## References

- Athanassoula E., Puerari I., Bosma A.: 1997, *MNRAS* **286**, 284  
 Berentzen, I., Heller, C.H., Shlosman, I., Fricke, K.J.: 1998, *MNRAS* **300**, 49  
 Berentzen, I., Heller, C.H., Athanassoula, E., Fricke, K.J.: 1999, in: *Dynamics of Galaxies and Galactic Nuclei*, SFB 328 Workshop, eds. W.J. Duschl & C. Einsel (Vol.2 of ITA series), 1999 a, *in press*.  
 Berentzen, I., Heller, C.H., Athanassoula, E., Fricke, K.J.: 1999 b, *in prep*.  
 Heller, C.H.: 1995, *ApJ* **455**, 252  
 Heller, C.H., Shlosman, I.: 1994 *ApJ* **424**, 84  
 Lynds, R., Toomre, A.: 1976 *ApJ* **209**, 382  
 Sellwood, J.A., Wilkinson, A.: 1993, *Rep. Prog. Phys.* **56**, 173

### Acknowledgements

We would like to thank Albert Bosma for interesting discussions, and J.C. Lambert and C. Theis for their computer assistance. The GRAPE 3Af special purpose computer in Kiel was financed under DFG grant Sp 345/5-1, 5-2. I.B. acknowledges support from DFG grant Fr 325/48-1, 48-2. C.H. acknowledges support from DFG grant Fr 325/39-1, 39-2. E.A would also like to thank the IGRAP, the INSU/CNRS and the University of Aix-Marseille I for funds to develop the grape facilities used for part of the calculations in this paper.

